ISSN: 0067-2904

Effect of the Gap Size between the Cathode and the Wehnelt Cylinder Bore on the Emittance of the Thermionic Electron Gun

Najia Abdullah Mohammed*, Abdullah Idrees Al-Abdullah
Department of Physics, College of Science, University of Mosul

Received: 25/7/2021 Accepted: 6/11/2021 Published: 30/8/2022

Abstract

This paper includes simulating an electron gun design to investigate the effect of the distance between the cathode and the Wehnelt cylinder bore on the quality of the ion beam emittance and to obtain the best distance of that geometrical factor. A study of a group of designs was conducted to find this distance. The SIMION8.0 program has been used to calculate the trajectories of the electrons with initial kinetic energy of (0.1 eV) and electron current of (1×10^{-12} A). The investigation also includes comparisons between the equipotential line trajectories for each design as well as the field distribution and the electron trajectories. The best emittance distance was concluded to be (3 mm).

Keywords: SIMION8.0 program, beam emittance, thermionic electron gun design.

تأثير حجم الفجوة بين الكاثود وفتحة اسطوانة ونلت على الانبعاثية في القاذف الالكتروني الحراري

ناجية عبدالله محمد*،عبدالله ادريس مصطفى
قسم الفيزياء، كلية العلوم، جامعة الموصل، الموصل ، العراق

الخلاصه

يتضمن هذا البحث عملية محاكاة لتصميم قاذف الكتروني حراري لدراسة المسافة بين الكاثود وعرض فجوة اسطوانة ونلت على جودة الحزمة الايونية والحصول على افضل مسافة لهذا العامل الهندسي، ومن خلال الدراسة تم تصميم مجموعة من القاذفات الالكترونية ذات اشكال متشابهة ومختلفة المسافة بين الكاثود وفتحة اسطوانة ونلت باستخدام برنامج (SIMION8.0) لحساب مسارات الالكترونات ذات الطاقة الحركية الابتدائية (0.1 eV)، وتيار الالكترون المتساوي في كل حالة وقيمته (1×10^{-12} A). تم في هذه الدراسة ايضا اجراء مقارنات بين مسارات خطوط تساوي الجهد لكل تصميم بالإضافة الى توزيع المجال ومسارات الالكترونات، وتم الحصول على افضل انبعاثيه للحزمة الالكترونية عند مسافة بين الكاثود وفتحة اسطوانة ونلت تساوي (3 mm).

1. Introduction

Electron guns are used in many vacuum electron devices to convert electrical power into an electron beam [1]. Electron beam devices have a variety of uses in different applications,

*Email: najia-scp86@student.uomosul.edu.iq

including communications, radar, industrial heating, and high-energy accelerators. Electron beams are also utilized for electron beam observation, lithography, and welding in medical and industrial X-ray devices, as well as in cathode ray guns for televisions and oscilloscopes. Many of these devices are essential for national security, science, and other purposes [2]-[3]-[4]. By heating a small cathode element, the cathode can generate a cloud of electrons through thermal emission; this is accelerated to form an electron beam.

Before a package is introduced into a system, it is critical to have complete information about its emittance, which is an important quantity to consider; it is the most important factor in producing a high-quality electron beam [5]. Electron guns can operate in two modes: continuous and pulsed. In electron guns, there are several methods for producing a burst of electrons. The most common methods are thermionic, photoelectric, and electric field emissions[6]. The cathode of electron guns has two important characteristics: emission continuity and uniformity [7]. The SIMION8.0 electron-beam ray-tracing tool was used in this study to model and optimize the electron gun's electron optics.

The purpose of this study is to determine the optimal distance between the cathode and the Wehnelt cylinder bore gap. This distance bore, has been found to equal (3 mm).

2. Theoretical Considerations

In the absence of a magnetic field, the electric field of an electron cannon is estimated using Poisson's equations, and electron trajectories are computed using Lorentz's force equations. The time-independent Maxwell's equations are the governing equations of the fields [6];

$$\nabla \cdot \mathrm{E} = \frac{\rho}{\epsilon_\circ} \tag{1}$$

Where: E denotes the electric field, ρ denotes the charge density, and ε_o denotes the vacuum permittivity. Determining the electron trajectories can be done using Lorentz force from the following equation:

$$\mathrm{F} = \frac{\mathrm{dp}}{\mathrm{dt}} = \mathrm{q}\,(\mathrm{E} + \mathrm{V} \times \mathrm{B}) \tag{2}$$

The magnetic field term is neglected due to its absence.

Commonly, the Child-Langmuir model is used for DC electron guns to find the electron flux j_e [8];

$$\mathrm{j}_e = \frac{4\pi\varepsilon_\circ}{9}\sqrt{\frac{2\mathrm{e}}{\mathrm{m_e}}}\frac{\mathrm{v}_o^{\frac{2}{3}}}{\mathrm{d}^2} \tag{3}$$

with d in meters and V_o in volts as the applied voltage. The practical expression is obtained by substituting values for the physical constants:

$$\mathrm{j_e} = 2.33 \times 10^{-6}\ {V_o}^{3/2}/\mathrm{d}^2 \tag{4}$$

The units are A/m^2 for d in meter.

For a radius < d/2, the extraction zone $A = \pi d^2/4$. An electron gun's greatest total current is:

$$\mathrm{j_e} = 2.33 \times 10^{-6}\frac{\pi}{4}\,V_o^{\frac{3}{2}} \tag{5}$$

3. Simulation Process

Using the SIMION8.0 program, the ion beam and its trajectories are simulated after the geometry of the electrodes and its potentials are determined. It uses the potential arrays, and by solving Laplace equation, the potential between the electrodes is determined. SIMION8.0 uses a refined method for analyzing the system. In this case, the array size represents boundary conditions. Laplace equation assumes there is no space charge effect and the boundary conditions are quite limited. Therefore, using Gauss theorem in a closed surface with no charge inside, which is shown in equation (6), we would have [9];

$$\nabla . E = 0 \tag{6}$$

For electrostatic case, the electric field is a gradient of a scalar field, which is shown in Equation (7)

$$\nabla v = \left(\frac{\partial v}{\partial x}\right)\hat{\mathrm{I}} + \left(\frac{\partial v}{\partial y}\right)\hat{\mathrm{j}} + \left(\frac{\partial v}{\partial z}\right)\hat{\mathrm{k}} = \mathrm{E} \quad (7)$$

From the two equations (6) and (7), Equation (8) is obtained:

$$\nabla^2 v = 0 \quad (8)$$

SIMION8.0 uses this equation to compute electrostatic and static magnetic potential fields. Whereas all electrostatic and static magnetic potential fields are constrained by Laplace equation to conform to the zero-charge volume density assumption (no space charge).

Poisson's equation allows space charge

$$\nabla^2 V = \nabla.\nabla \mathrm{V} = -\mathrm{p}/\mathrm{e} \quad (9)$$

A non-zero charge volume density is allowed by Poisson's equation (space-charge). When the density of ions is high enough (high beam currents), the electrostatic potential fields are significantly distorted by their presence. To estimate potential fields in these circumstances, Poisson's equation (rather than Laplace's) should be used. Poisson solutions to field equations are not supported by SIMION8.0. Charge repulsion methods, on the other hand, are used to estimate certain types of space charge and particle repulsion effects [10]-[11]-[12].

3.1. The Beam Emittance

Emittance is an area or volume in the phase space of the particles, and it is the property of the particle beam that characterizes its size for each spatial direction. There are two types of space variables, the phase space variables, which are (x, p_x), (y, p_y) and (z, P_z) for a particle with time as the independent variable. These coordinates correspond to the momentum components of the particle with position, and these coordinates are taken as errors of momentum and position if the particle is perfect [13].

Emittance is used to describe a beam because it is opposite to the physical dimensions of the beam and it varies according to each location in the accelerators. Emittance is invariant in the absence of dissipative or cooling forces. As this case is the simplest, it will be used for examples and discussion in this study. Liouville's theory states that the motion of charged particles by the effect of conservative fields creates local number density in the space phase of the six-dimension as a conserved quantity [14]. If a group of particles' transverse components of motion is mutually independent in space, they are also mutually independent in the orthogonal phase space planes (x, p_x), (y, p_y) and (z, P_z), with the corresponding phase space areas conserved separately. The emittance of the beam is proportional to the transverse phase space areas, which are thus conserved if cylindrical symmetry can be assumed. Consider ions passing through (x, y) related to r at a certain point on the z-axis, momentum component P_z approximately equals total particle momentum p [15].

The beam emittance values have been calculated at the splat location in this research converted to Lua scripts written by [10].

3.2. Ion Beam Diameter

The simulation includes studying the diameter of the ion beam and then studying its relationship to the separation distance between the cathode and the Wehnelt cylinder bore. The best ion beam diameter has been conceded at the minimum value.

4. The Computation analysis and Results

4.1. The Electron Gun Design

The typical electron gun shape and its geometrical parameters are shown in Figure 1. For each design the value of the distance between the cathode and Wehnelt cylinder bore was taken in the present computation as S= 0, 1, 2, 3, 4, 5, 6, 7, 8, 9 & 10 mm. It can be seen that the distance between the anode and the Wehnelt cylinder is (20 mm), the internal anode diameter is (20 mm), and the thickness of the anode is (2 mm),as for the Wehnelt cylinder the inner diameter is (10 mm) and the outer thickness is (2 mm).

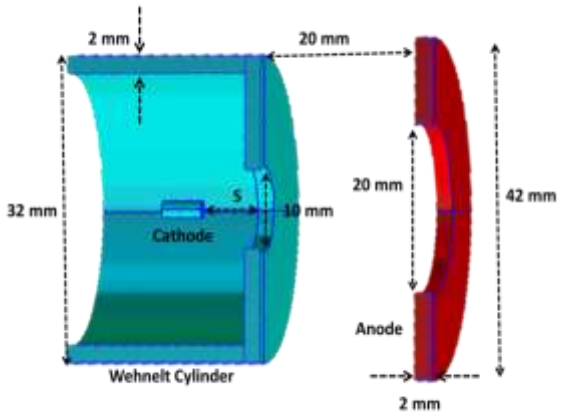

Figure 1- The geometrical dimensions of the thermionic electron gun design

The electron gun has three electrodes denoted V1(Cathode), V2(Wehnelt cylinder) and V3(Anode) as shown in Figure 1. The electrostatic scalar potential for each electrode is equal to (-10, -10 & 0 kV), respectively.

4.2. The Electric Field

The variation of the electric field for the cases of S= 1, 3, 5 & 7 mm has been calculated and demonstrated in Figure 2. This figure shows that there is enormous variation of the field at the location of the gap between the cathode and the Wehnelt cylinder bore where (x=18-32 mm), while almost coincide at the other locations.

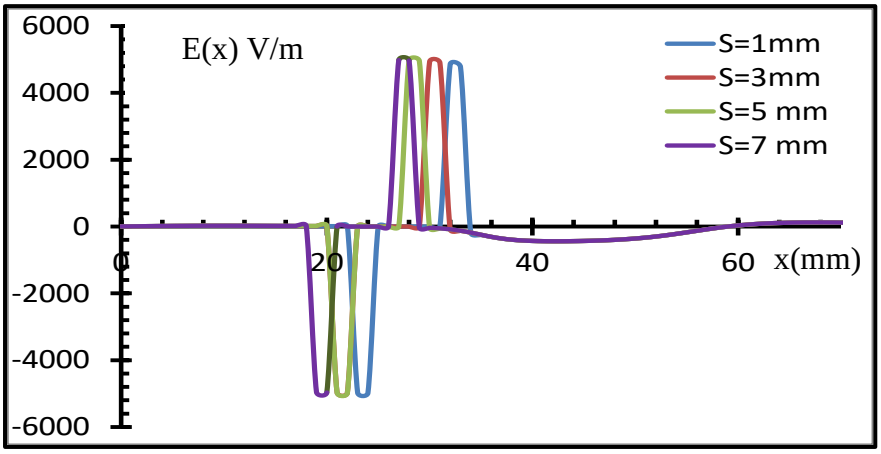

Figure 2- Comparison of the electric field with distance for S= 1, 3, 5 & 7 mm)

4.3. The Electrostatic Potential

The electrostatic potential for each value of (S) has been calculated and compared in Figure 3 for the value of (S= 1, 3, 5 & 7 mm). it has been noticed that there is enormous variation of the potential at the location of the gap between the cathode and the Wehnelt cylinder bore for x=20-32 mm, while almost coincide at the other locations.

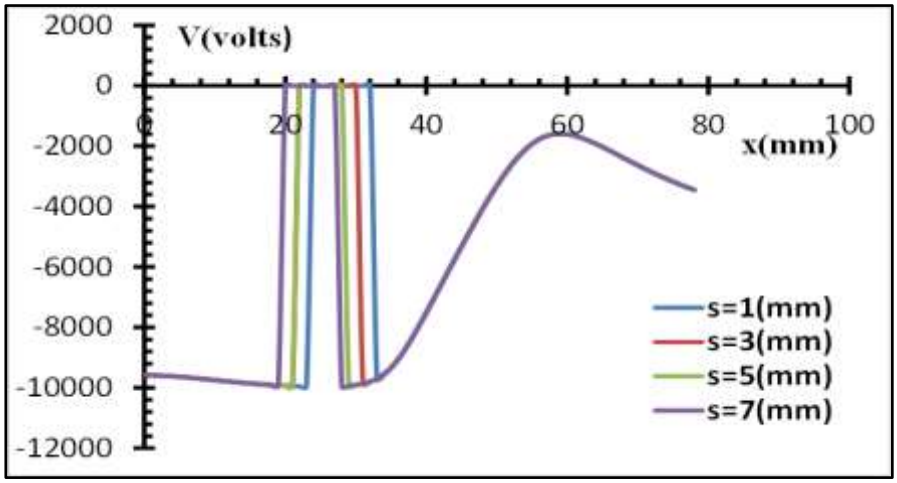

Figure 3-Comparison of the electric potentials with distance for S= 1, 3,5 & 7 mm)

4.4. The Equipotential Lines

The equipotential lines contours and electron beam trajectories were calculated and were noted to overlap for the values of S= 1, 3, 5 & 7 mm, as shown in Figure 4. This figure shows that the distance between the Wehnelt cylinder bore and the cathode has a great effect on electron beam trajectories.

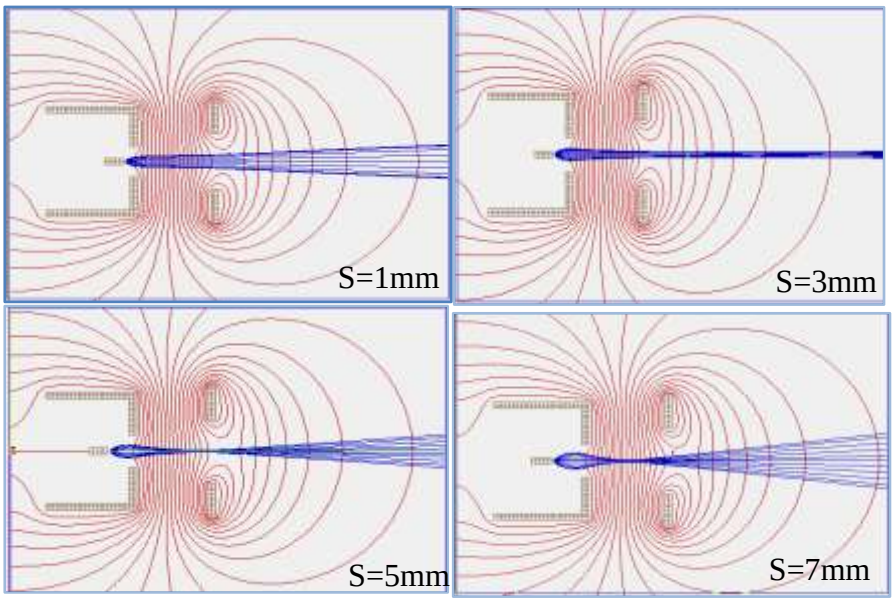

Figure 4- Comparison between the equipotential lines contours and electron beam trajectories for the system (S= 1, 3, 5 & 7 mm)

The results obtained by the ion beam trajectory is shown in Figure 5, the SIMION8.0 program provides a 3D view of the potential array and the equipotential lines with the electron beam trajectories. This figure shows the results for the case of S=3, 4 & 5 mm and the voltage applied to V1, V2, and V3 are equal to (-10, -10 & 0 kV), respectively.

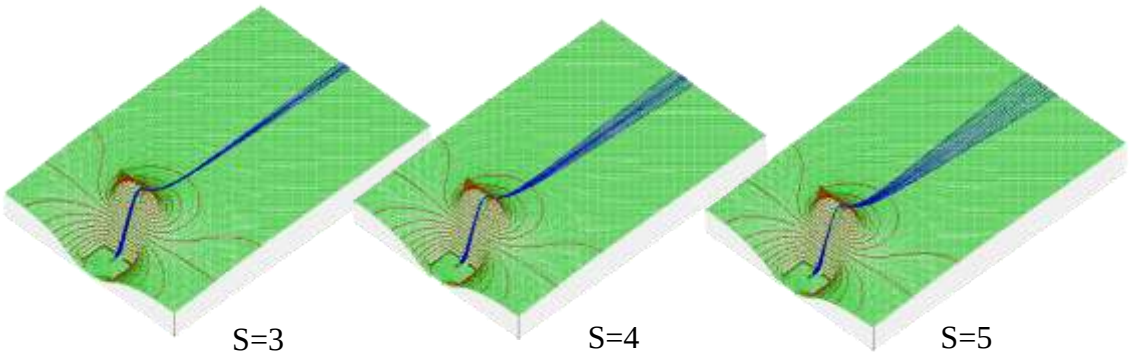

Figure 5- The potential array in 3D view of the equipotential lines with the electron beam trajectories for the case of (S= 3, 4 & 5 mm) and **and the voltage applied to** V1, V2 and V3, are equal to (-10, -10 & 0 kV) respectively

4.5. Trajectories of the Beam

Comparison between the trajectories of the electron beam for each value of (S) is demonstrated in Figure 6. This figure shows that the geometrical factor (S) has a large effect on the electron beam trajectories. Before deciding which value of S has better performance, both the electron beam and emittance must be calculated.

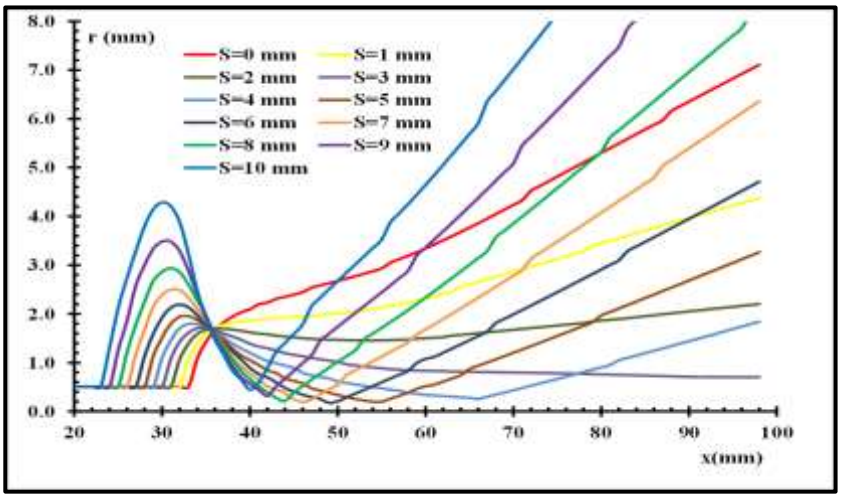

Figure 6- The comparison between trajectories of the beam of the systems at different values of S(0, 1, 2, 3, 4, 5, 6, 7, 8, 9 & 10 mm)

4.6. The Ion Beam Diameter

The diameter of the electron beam was also calculated by the SIMION8.0 program, and the simulation results are shown in Figure 7, which shows that the best value of the beam diameter (r) was achieved at S=5 mm, where the best diameter was considered at the middle of its stable range (S=4-8 mm).

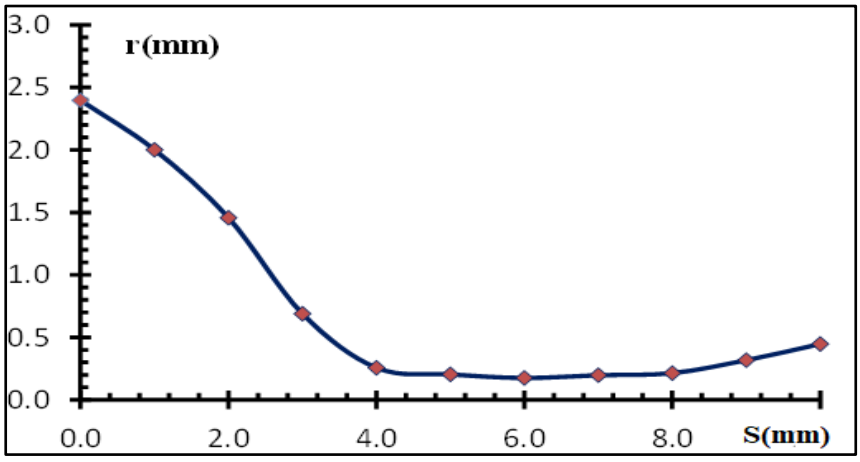

Figure 7- The relationship between the ion beam diameter and distance S(0, 1, 2, 3, 4, 5, 6, 7, 8, 9 & 10 mm)

4.7. The Beam Emittance

Figure 8 shows the relationship between the beam emittance and the distance between cathode and Wehnelt cylinder bore. From the figure, it is noted that the best emittance was at a distance of (3 mm). The value of the best emittance was considered at the middle of its stable range (S=2-4 mm).

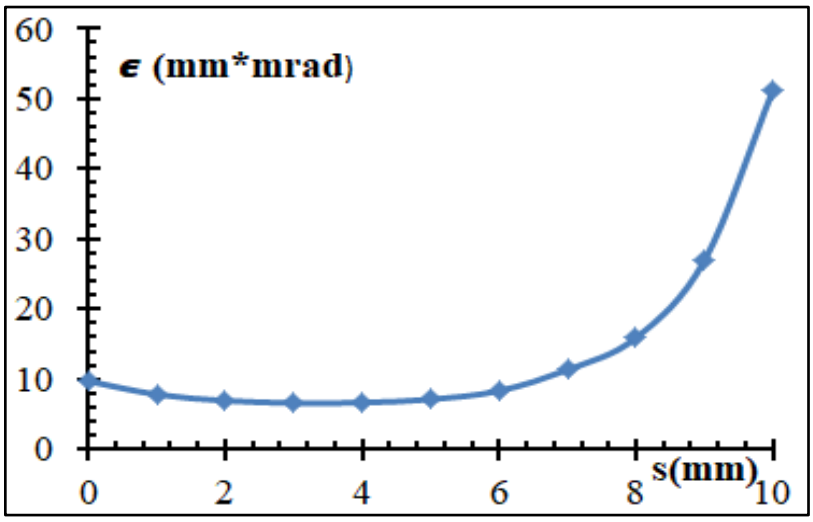

Figure 8- The relationship between emittance and distance for each S(0, 1, 2, 3, 4, 5, 6, 7, 8, 9 & 10 mm)

A conclusion from Figures (7 & 8) can be reached that the optimal distance between the cathode and the Wehnelt cylinder bore is (4 mm) for the present design.

6. Conclusions

The simulation results showed that the optimal ion beam formation process depended greatly on the distance between the cathode and the Wehnelt cylinder bore. It also depended on the electrical potential of both the cathode and the Wehnelt cylinder bore. Incorrect electrode geometry and voltage would cause the particle trajectory to be non-linear and not focused and can affect the beam emittance or ion beam diameter spot. This study proved that the minimum electron beam diameter occurred at (5 mm) distance between the cathode and the Wehnelt

cylinder bore. At this distance, the best emittance beam was produced. Therefore, the best compromised value of the distance is considered which is (4 mm).

References

[1] S. A. Molokovsky, and Sushkov. *Intense electron and ion beams. Heidelberg, Germany: Springer-Verlag Berlin*, 2005.

[2] M. Abdelrahman and S. Zakhary, "Simulation studies for ion beam extraction systems," *Brazilian Journal of Physics*, vol. 39, pp. 275-279, 2009.

[3] T. Peter and A. Brady, A thesis submitted in partial fulfillment of the requirements for the degree of bachelor of science", Houghton College, USA, 2004.

[4] T. Tuohimaa, "Liquid-jet-target microfocus x-ray sources: electron guns, optics and phase-contrast imaging," KTH, 2008.

[5] A. A. El-Saftawy, A. Elfalaky, M. S. Ragheb, and S. G. Zakhary, "Numerical Simulation of Beam Formation and Transport in an Electron Gun for Different Applications," *Journal of Nuclear and Particle Physics*, vol. 2, no. 5, pp. 126-131, 2012.

[6] M. Hoseinzade, M. Nijatie, and A. Sadighzadeh, "Numerical simulation and design of a thermionic electron gun," *Chinese Physics C*, vol. 40, no. 5, p. 057003, 2016.

[7] M. Sedlacek, *Electron physics of vacuum and gaseous devices*. Wiley-VCH, 1996.

[8] I. G. Brown, *The physics and technology of ion sources*. John Wiley & Sons, 2004.

[9] S. Adabiah, S. Munawaroh, and S. Haniah, "Simulation study for ion beam extraction of 150 keV/2mA ion implantor by using SIMION 8.1," in *Journal of Physics: Conference Series*, 2020, vol. 1436, no. 1: IOP Publishing, p. 012123.

[10] D. J. Manura and D. A. Dahl, SIMION Version 8.0/8.1 User Manual, Scientific Instrument Services, Inc., 2008.

[11] D. J. Manura and D. A. Dahl, SIMION Version 8.0/8.1 User Manual, Scientific Instrument Services, Inc., 2011.

[12] D. J. Manura and D. A. Dahl, SIMION Version 8.0/8.1 User Manual, Scientific Instrument Services, Inc., 2020.

[13] D. A. Edwards and M. J. Syphers, *An introduction to the physics of high energy accelerators*. John Wiley & Sons, 2008.

[14] M. Abdelrahman, "Simulation Study for Electron Gun Using Simion Computer Program," *Journal of Asian Scientific Research*, vol. 3, no. 3, pp. 275-285, 2013.

[15] T. Green, "Simulation studies for ion beam," *IEEE Nucl. Sci. NS*, vol. 23, pp. 918-925, 1976.